Medscape
EDUCATION

Continuing Medical Education:

Bruch's membrane opening-based optical coherence tomography of the optic nerve head: a useful diagnostic tool to detect glaucoma in macrodiscs

P Enders[1], F Schaub[1], W Adler[2], MM Hermann[1],
TS Dietlein[1], C Cursiefen[1] and LM Heindl[1]

Release date: 26 January 2018; Expiration date: 26 January 2019

JOINTLY ACCREDITED PROVIDER™
INTERPROFESSIONAL CONTINUING EDUCATION

In support of improving patient care, this activity has been planned and implemented by Medscape, LLC and Springer Nature. Medscape, LLC is jointly accredited by the Accreditation Council for Continuing Medical Education (ACCME), the Accreditation Council for Pharmacy Education (ACPE), and the American Nurses Credentialing Center (ANCC), to provide continuing education for the healthcare team.

Medscape, LLC designates this Journal-based CME activity for a maximum of *1.00 AMA PRA Category 1 Credit(s)™*. Physicians should claim only the credit commensurate with the extent of their participation in the activity.

All other clinicians completing this activity will be issued a certificate of participation. To participate in this journal CME activity: (1) review the learning objectives and author disclosures; (2) study the education content; (3) take the post-test with a 75% minimum passing score and complete the evaluation at **www.medscape.org/journal/eye**; (4) view/print certificate.

Learning Objectives

Upon completion of this activity, participants will be able to:

1. Compare morphometric measurements and diagnostic performance for glaucoma detection in macrodiscs by Bruch's membrane opening-based spectral domain-optical coherence tomography (SD-OCT) and margin-based confocal scanning laser tomography (CSLT) of the optic nerve head, based on a case-control, cross-sectional study

2. Assess correlation of SD-OCT and CSLT for glaucoma detection with visual field function

3. Determine the clinical implications of these findings regarding morphometric measures in macrodiscs of glaucomatous and nonglaucomatous eyes

Authors/Editors disclosure information

Andrew J. Lotery has disclosed the following relevant financial relationships: Served as an advisor or consultant for:

Bayer HealthCare Pharmaceuticals; Gyroscope Therapeutics; Roche. Owns stock, stock options, or bonds from: Gyroscope Therapeutics

Philip Enders has disclosed no relevant financial relationships.
Friederike Schaub has disclosed no relevant financial relationships.
Werner Adler has disclosed no relevant financial relationships.
Manuel M. Hermann has disclosed no relevant financial relationships.
Thomas Dietlein has disclosed no relevant financial relationships.
Claus Cursiefen has disclosed no relevant financial relationships.
Ludwig M. Heindl has disclosed no relevant financial relationships.

Journal CME author disclosure information.

Laurie Barclay has disclosed the following relevant financial relationships: owns stock, stock options, or bonds from: Alnylam; Biogen; Pfizer Inc.

Bruch's membrane opening-based optical coherence tomography of the optic nerve head: a useful diagnostic tool to detect glaucoma in macrodiscs

P Enders[1], F Schaub[1], W Adler[2], MM Hermann[1], TS Dietlein[1], C Cursiefen[1] and LM Heindl[1]

CLINICAL STUDY

Abstract

Purpose To compare Bruch's membrane opening (BMO)-based spectral domain optical coherence tomography (SD-OCT) and margin based confocal scanning laser tomography (CSLT) of the optic nerve head (ONH) to visual field function in large optic discs (macrodiscs) and to assess performance for glaucoma detection.

Methods In a case–control, cross-sectional study, 125 eyes of 125 patients with disc size $> 2.45\ mm^2$, thereof 44 glaucoma and 11 ocular hypertension (OHT) patients and 70 healthy controls underwent SD-OCT and CSLT examination, visual field testing and clinical evaluation. Mean outcome measures BMO-based minimum rim width (BMO-MRW), retinal nerve fiber layer thickness (RNFLT) in SD-OCT, and rim area measured in CSLT were compared and correlated to visual field function.

Results All participants had a mean disc area of $2.91 \pm 0.38\ mm^2$ in CSLT and a BMO area of $2.45 \pm 0.39\ mm^2$ ($r = 0.76; P < 0.001$). In glaucoma patients, visual field mean deviation was -10.0 ± 6.1 dB. Global BMO-MRW correlated better to visual field function (Spearman's Rho (ρ) = 0.71; $P < 0.001$) than RNFLT ($\rho = 0.52; P < 0.001$) and CSLT rim area ($\rho = 0.63$; $P < 0.001$). BMO-MRW was significantly decreased with higher visual field loss ($P < 0.001$). In ROC analysis, diagnostic power to differentiate glaucoma patients and healthy controls was highest for BMO-MRW (Area under curve, AUC = 0.96; sensitivity at 95% specificity = 82%). Rim area in CSLT (AUC = 0.91; sensitivity = 61.0%; $P = 0.04$) and RNFLT (AUC = 0.89; sensitivity = 61%; $P = 0.01$) were significantly less powerful.

Conclusions In macrodiscs, BMO-MRW has the best diagnostic power to discriminate glaucoma patients from normal controls compared to RNFLT and rim area in CSLT. Additionally, BMO-MRW seems to reflect the structure-function relationship better than the other two parameters.

Introduction

In very small or very large optic nerve heads diagnosis of glaucoma presents a major challenge for the clinician. In large optic discs, while the number of ganglion axons is equivalent or even higher compared to 'regular' sized discs, the neuroretinal rim in funduscopy seems thinned. Reason for this includes, that patients with large optic discs present physiologically a large irregular excavation of the optic nerve head.[1–3]

Morphometric analysis of the optic nerve head (ONH) and visual field testing represent the major keystones in diagnosis, treatment planning and follow-up of glaucoma patients.

Bruch's membrane opening minimum rim width (BMO-MRW) as well as retinal nerve fiber layer thickness (RNFLT) analysis of the optic nerve head by Bruch's membrane opening (BMO) based spectral domain optical coherence tomography (SD-OCT) becomes increasingly

[1]Department of Ophthalmology, University Hospital of Cologne, Cologne, Germany

[2]Department of Medical Informatics, Biometry and Epidemiology, Friedrich-Alexander University Erlangen-Nuremberg, Erlangen, Germany

Correspondence:
P Enders, Department of Ophthalmology, University Hospital of Cologne, Kerpener Str 62, Cologne 50924, Germany
Tel: +49 022 1478 4308;
Fax: +49 022 1478 3526.
E-mail: Philip-enders@web.de

available to clinicians and proposes advantages compared to the previous clinical standard of morphometric optic nerve head analysis, confocal scanning laser tomography (CSLT) measurement.[4–6] SD-OCT technique allows calculation of neuroretinal rim parameters based on the area of a surface extending from Bruch's membrane opening (BMO) to the inner limiting membrane (ILM) and increasing validity by extending imaging to sub-surface structures.[7] Besides other global and localized RNFLT measurements, global and sectorial mean minimum rim width parameters based on BMO (BMO-MRW) have been introduced and evaluated.[4,7–14]

Correlation of morphometric ONH parameters and visual field function has been evaluated in numerous studies.[4,15–21] Analyses aimed to explore individual correlation of morphometric ONH parameters as neuronal rim width to visual field parameters as mean deviation and to derive, if possible, a forecast of visual field defects based to ONH.

Qualification and quantification of the relation between structural damage to the ganglion axons in the optic nerve head and the functional, perimetric damage have been principal aim in glaucoma research. A recent study by Muth *et al*[22] analyzed structure-function relationship between SD-OCT of the ONH and visual field testing in 46 eyes with random size of the optic disc.

The study contributes to the current effort to compare margin based rim area measurements from CSLT with BMO based measurements from SD-OCT. Recently, morphometric data for eyes with non-glaucomatous macrodiscs has been published by our group.[23] Malik *et al* recently published an analysis on the diagnostic power in myopic discs; this group assessed the diagnostic power of one-dimensional SD-OCT-based morphometric parameters in microdiscs independent from refractive status.[24,25]

The purpose of the present study is to assess the diagnostic power to detect glaucoma by OCT diagnostics of glaucomatous large optic nerve heads, so called macrodiscs (disc size > 2.43 mm^2 in CSLT). Further goal was to evaluate structure-function relationship of OCT-based morphometric data along different classifications of the glaucomatous visual field. Especially for large optic nerve heads, sufficient data is still missing.

Materials and methods

Data for this single-center retrospective analysis was acquired from September 2014 to March 2016 at the Department of Ophthalmology, University Clinic of Cologne, Germany. All consecutive patients receiving both CSLT as well as SD-OCT measurements of the optic nerve head were screened for size of the optic nerve head. Both measurements of one individual took place on the

same day. For visual field testing a time gap of ± 4 weeks was considered acceptable for inclusion.

Additional parameters were collected from patients' files: Diagnosis of glaucoma, previous anti-glaucomatous surgery, best corrected visual acuity (BCVA), visual field testing, intraocular pressure (IOP), topical medication, and medical history of the eyes. IOP has been assessed by corneal rebound tonometry (Icare tonometer TA01i) and by Goldmann tonometry in adults and children, respectively.

Eyes with a large optic nerve head of more than 2.43 mm^2 in CSLT were included in this study. This threshold was set by exceeding the upper limit for the normative collective in CSLT according to software version 3.1.0.2. The exclusion criteria were: visual field loss because of other etiologies than glaucoma, unsatisfactory image quality in CSLT, SD-OCT, or in visual field testing, and BCVA > 0.4 logMAR. Only patients with primary open-angle glaucoma including pseudoexfoliation and pigmentary forms were included. For non-glaucomatous individuals, a mean deviation of better than − 3 dB was required, following an outside expert guidance in peer review of the previous analysis on non-glaucomatous macrodiscs.[23] If multiple data points at different time points were available, then the examination with the best imaging quality indicators was used. If both eyes fulfilled all inclusion criteria and no exclusion criteria, the eye with the larger disc size was selected.

One hundred twenty five eyes of 125 patients could be included in this study out of a source database of 220 eyes with macrodiscs. A total of 14 eyes lacked sufficient clinical information or quality of visual field testing, 28 eyes of non-glaucomatous controls exceed the defined limit for mean deviation in visual field of − 3 dB. Further, 53 eyes have been excluded being the fellow of a patient with eligibility of both eyes.

Patients have been classified into three different diagnostic groups according to the 4th Edition of Guidelines of the European Glaucoma Society (EGS, 2014): (1) Glaucoma patients; (2) patients with ocular hypertension (OHT); and (3) individuals with no suspicion of glaucoma.[26] In EGS guidelines, glaucomas are progressive optic neuropathies that have in common characteristic morphological changes at the optic nerve head and retinal nerve fibre layer in the absence of other ocular disease of congenital anomalies. Progressive ganglion cells death and visual field loss are associated with the changes. For glaucoma patients included in this study, beginning changes in visual field assessment were required.

CSLT and SD-OCT examinations were executed by Heidelberg Engineering Retina Tomograph III and Spectralis SD-OCT (Heidelberg Engineering GmbH,

Table 1 Epidemiological and baseline data

	Glaucoma patients	Patients with ocular hypertension (OHT)	Controls
N	44	11	70
Gender n (%)			
Men	21 (47.7)	7 (63.6)	32 (45.7)
Women	23 (52.3)	4 (36.4)	38 (54.3)
Age (years)			
Mean (SD)	65.0 (±11.0)	51.0 (±12.4)	38.2 (±25.0)
Median	65.0	49.0	33.5
Range	55 to 75	33 to 77	3 to 86
Eye n (%)			
Right	20 (45.5)	5 (45.5)	34 (48.6)
Left	24 (54.5)	6 (54.5)	36 (51.4)
BCVA (logMAR)			
Mean (SD)	0.2 (±0.25)	0.05 (±0.09)	0.03 (±0.1)
Median	0.1	0.0	0.0
IOP (mmHg)			
Mean (SD)	17.9 (±7.5)	15.0 (±3.7)	17.2 (±3.4)
Median	17.0	14.0	18.0
Mean deviation (dB) of 30/2 visual field testing			
Mean (SD)	− 10.0 (±6.1)	− 1.1 (±0.8)	− 0.6 (±1.6)
Median	− 8.8	− 1.1	− 0.9
Range	− 24.9 to − 0.9	− 2.1 to 0.2	− 2.8 to 5.3
Aulhorn classification or glaucomatous scotoma n (%)		n/a	n/a
Degree 1	12 (27.3)		
Degree 2	12 (27.3)		
Degree 3	10 (22.3)		
Degree 4	8 (18.2)		
Degree 5	2 (4.5)		
Hodapp classification for glaucomatous scotoma n (%)		n/a	n/a
Stage 1	14 (31.8)		
Stage 2	15 (34.1)		
Stage 3	15 (34.1)		
Disc size in CSLT (mm^2)			
Mean (SD)	2.71 (±0.80)	2.95 (±0.41)	2.98 (±0.41)
Range	2.44–3.72	2.50–3.83	2.45–4.23
BMO area in SD-OCT (mm^2)			
Mean (SD)	2.71 (±0.80)	2.40 (±0.44)	2.50 (±0.40)
Range	2.44–3.72	1.16–3.04	1.81–3.35

Abbreviations: BMO, Bruch's membrane opening; CSLT, confocal scanning laser tomography; SD-OCT, spectral domain optical coherence tomography.

Heidelberg, Germany) following standard operating procedures. Two independent evaluators (EP, SF) assessed image quality and—in CSLT—defined the disc margin manually; threshold for the SD of the CSLT topography was set < 40 μm. SD-OCT data included comprised an image quality index of > 15 dB. In case of a significant discrepancy between the disc margins drawn by the operators, the images were reevaluated until consensus was achieved. The neuroretinal rim was calculated automatically by using the CSLT standard reference plane. SD-OCT imaging was performed with a commercially available Heidelberg Spectralis device. A light source of 870 nm was used according to standard imaging procedure. The scanning pattern was centered on the optic disc with radial equidistance (24-high resolution 15° radial scans, each averaged from 27 B-scans). The examiners controlled the centration of the scan to the optic disc and corrected errors in detection of internal limiting membrane (ILM) and Bruch's membrane opening. OCT-based parameters were calculated by the device operating software tool provided by Heidelberg Engineering, including a data export batch provided by the manufacturer.

Visual field testing at the site was performed using a Octopus 101 visual field analyzer (Haag-Streit AG, Koeniz, Switzerland) with a 30/2 TOP white-on-white standard pattern and analyzed by Peridata 3.1. Age and refraction matching lens correction was applied, visual field testing was performed separately for both eyes. Thresholds for reliability were set at ≤ 30% for false positive and false-negative answers as well as ≤ 20% for fixation losses.

Visual field results were screened manually for glaucomatous scotoma and classified according to Aulhorn and Karmeyer.[27–29] Additionally, patients were classified based on a simplified modification of the Hodapp–Anderson–Parrish system:[30] Patients were divided into three groups depending on their global mean deviation in perimetry as output parameter. (MD-G). A more negative number indicates a higher loss in function. The groups are: early glaucoma (MD-G equal to or above − 6 dB), moderate glaucoma (MD-G below − 6 dB but equal to or above − 12 dB), and severe glaucoma (MD-G below − 12 dB).

According to national medical regulations on retrospective single center clinical studies Ethics Committee of the University of Cologne ruled that approval was not required for this study. All tenets of the declaration of Helsinki have been regarded.

Statistical analysis was performed by SPSS Version 22.0 (IBM Corp. Armonk, NY, USA), the statistical programming language R V3.2.2 (R Foundation for Statistical Computing, Vienna, Austria and by MedCalc Statistical Software Version 16.4.3 (MedCalc Software

Bvba, Ostend, Belgium; https://www.medcalc.org; 2016). Pearson correlation coefficient *r* and Spearman rank correlation coefficient ρ were used depending on normal distribution of parameters. Diagnostic power was assessed by receiver operating characteristic (ROC) analysis and tested for statistically significant difference with DeLong test. Threshold for statistical significance was set at $P < 0.05$. Threshold for statistical significance was set at $P < 0.05$. Holm–Bonferroni procedure was used to correct *P*-values for multiple testing.[31]

Results

Out of 125 eyes of 125 patients included in this study with macrodiscs, glaucoma has been diagnosed in 44 (35.2%) patients; ocular hypertension was present in 11 (8.8%), while 70 (56.0%) individuals had clinically no suspicion of glaucoma. Table 1 summarizes the epidemiologic characteristics and baseline data of the included eyes clustered by diagnoses.

Eyes with macrodiscs and glaucoma

In 44 eyes with glaucomatous macrodiscs, mean disc size ($\pm$ SD) in CSLT was 2.71 ± 0.80 mm^2 (range, 2.44–3.72 mm^2) and BMO area was 2.41 ± 0.34 mm^2 (range, 1.93–3.42 mm^2).

Mean BMO-MRW was 124.3 ± 42.5 μm (range, 59.87–242.17 μm), mean RNFLT was 54.41 ± 15.4 μm (range, 27–102 μm), and mean rim area in CSLT was 0.86 ± 0.36 mm^2 (range, 0.23–1.73 mm^2). Correlation between disc size in CSLT and BMO area was significant ($r = 0.71$; $P < 0.001$).

Pearson correlation coefficient between BMO-MRW and mean rim area in CSLT was $r = 0.80$ ($P < 0.001$), and between RNFLT and BMO-MRW $r = 0.75$ ($P < 0.001$), respectively. Correlation between RNFLT and mean rim area in CSLT was smaller with $r = 0.57$ ($P < 0.001$). Table 2 displays the morphometric data with global and sectorial analyses.

In Spearman non-parametric correlation, the parameter BMO-MRW correlates better to visual field function parameter mean deviation ($\rho = 0.71$; $P < 0.001$) than the two other examined morphometric factors RNFLT ($\rho = 0.52$; $P < 0.001$) and rim area of CSLT ($\rho = 0.63$; $P < 0.001$). Mean BMO-MRW values were evaluated along the two introduced visual field classifications in glaucoma. In Hodapp-Anderson-Parrish system, mean BMO-MRW decreased significantly from 157.88 ± 47.2 μm in stage 1 to 114.64 ± 29.5 μm in stage 2 and 102.71 ± 29.9 μm in stage 3. ($P = 0.002$, Jonckheere–Terpstra test; Figure 1). In degrees of Aulhorn classification, mean minimum rim width in OCT decreased from 162.65 ± 47.3 μm in degree 1 to 118.74 ± 26.0 μm in degree 2, 100.88 ± 21.6 μm in degree 3,

Table 2 Confocal scanning laser tomography (CSLT) and spectral domain optical coherence tomography (SD-OCT) based neuroretinal rim parameters including six optic nerve sectors

	Gobal	*Nasal*	*Nasal superior*	*Nasal inferior*	*Temporal*	*Temporal superior*	*Temporal inferior*
Glaucoma							
BMO-MRW, μm (SD-OCT)	124.33 ($\pm$42.53)	135.91 ($\pm$53.03)	139.52 ($\pm$58.56)	158.78 ($\pm$63.58)	110.57 ($\pm$43.98)	97.07 ($\pm$55.68)	119.38 ($\pm$55.07)
RNFLT, μm (SD-OCT) (SD)	54.10 ($\pm$15.43)	44.52 ($\pm$18.40)	60.86 ($\pm$23.99)	54.95 ($\pm$23.59)	51.02 ($\pm$18.63)	66.11 ($\pm$24.47)	71.09 ($\pm$35.06)
Rim area, mm^2 (CSLT)	0.86 ($\pm$0.36)	0.28 ($\pm$0.24)	0.14 ($\pm$0.07)	0.14 ($\pm$0.07)	0.13 ($\pm$0.06)	0.08 ($\pm$0.06)	0.10 ($\pm$0.06)
Ocular hypertension							
BMO-MRW, μm (SD-OCT)	226.38 ($\pm$38.37)	252.47 ($\pm$53.77)	255.61 ($\pm$72.03)	306.09 ($\pm$68.21)	171.80 ($\pm$26.16)	223.12 ($\pm$53.11)	257.69 ($\pm$54.22)
RNFLT, μm (SD-OCT)	72.27 ($\pm$17.19)	53.55 ($\pm$16.87)	76.00 ($\pm$26.73)	72.36 ($\pm$30.00)	57.91 ($\pm$10.28)	107.64 ($\pm$27.34)	117.45 ($\pm$26.59)
Rim area, mm^2 (CSLT)	1.66 ($\pm$0.39)	0.46 ($\pm$0.15)	0.25 ($\pm$0.08)	0.26 ($\pm$0.06)	0.26 ($\pm$0.09)	0.21 ($\pm$0.05)	0.23 ($\pm$0.07)
Normal controls							
BMO-MRW, μm (SD-OCT)	243.08 ($\pm$44.07)	248.28 ($\pm$53.84)	258.94 ($\pm$65.44)	301.10 ($\pm$62.81)	192.72 ($\pm$41.32)	232.98 ($\pm$56.47)	278.36 ($\pm$52.80)
RNFLT, μm (SD-OCT)	82.69 ($\pm$15.76)	66.90 ($\pm$17.26)	92.26 ($\pm$28.66)	87.17 ($\pm$25.85)	62.81 ($\pm$12.97)	113.43 ($\pm$24.58)	126.94 ($\pm$25.28)
Rim area, mm^2 (CSLT)	1.54 ($\pm$0.34)	0.46 ($\pm$0.11)	0.22 ($\pm$0.06)	0.24 ($\pm$0.06)	0.23 ($\pm$0.09)	0.18 ($\pm$0.06)	0.20 ($\pm$0.07)

Abbreviations: BMO-MRW, Bruch's membrane opening minimum rim width; CSLT, confocal scanning laser tomography; ONH, optic nerve head; RNFLT, retinal nerve fiber layer thickness; SD-OCT, spectral domain optical coherence tomography.
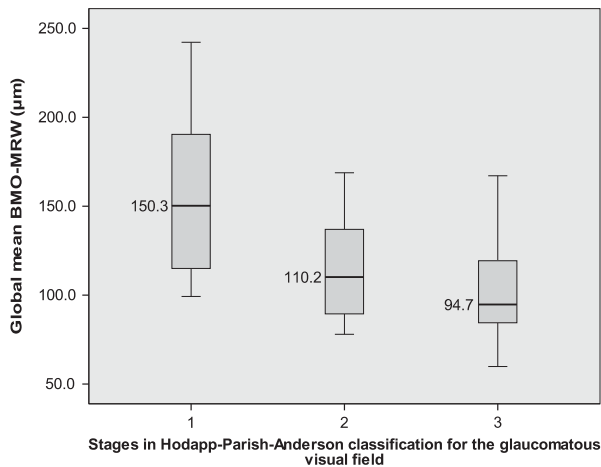
Figure 1 Global Bruch's membrane opening-based minimum rim width in visual field classifications: Hodapp stages. Note: boxplot graphs display global Bruch's membrane opening-based minimum rim width (BMO-MRW) medians and ranges for three different stages of the Hodapp classification for glaucomatous visual field defects.

Figure 2 Global Bruch's membrane opening-based minimum rim width in visual field classifications: Aulhorn degrees. Note: boxplot graphs display global Bruch's membrane opening-based minimum rim width (BMO-MRW) medians and ranges for different degrees of glaucomatous visual field defects according to Aulhorn classification.

$106.58 \pm 38.5\ \mu$m in degree 4 and $94.27 \pm 17.7\ \mu$m in degree 5. ($P < 0.001$, Jonckheere–Terpstra test; Figure 2).

Eyes with macrodiscs and ocular hypertension

In 11 eyes with macrodiscs and ocular hypertension, mean disc size in CSLT was $2.95 \pm 0.41\ \text{mm}^2$ (range, 2.50–3.83 mm^2), mean BMO area was $2.40 \pm 0.44\ \text{mm}^2$ (range, 1.16–3.04 mm^2). Mean global BMO-MRW was $226.38\ \mu$m (range, 177.9–302.4 μm), mean RNFLT was $72.3 \pm 15.2\ \mu$m (range, 49–106 μm), and mean rim area in CSLT was $1.66 \pm 0.39\ \text{mm}^2$ (range, 1.22–2.20 mm^2). Disc area in CSLT and BMO correlated strongly ($r = 0.88$, $P < 0.001$). Table 2 displays the morphometric data with global and sectorial analyses.

Normal controls with macrodiscs

In 70 eyes of non-glaucomatous controls, mean disc size in CSLT was $2.98 \pm 0.41\ \text{mm}^2$ (range, 2.45–4.23 mm^2), and mean BMO area was $2.50 \pm 0.40\ \text{mm}^2$ (range, 1.81–3.35 mm^2). Mean global BMO-MRW was $243.1 \pm 44.1\ \mu$m (range, 120.1–350.0 μm), mean RNFLT was $82.7 \pm 15.8\ \mu$m (range, 37–110 μm) and mean rim area in CSLT was $1.54 \pm 0.34\ \text{mm}^2$ (range, 0.74–2.51 mm^2).

Disc area in CSLT and BMO area correlated strongly ($r = 0.83$, $P < 0.001$). Table 2 displays the morphometric data with global and sectorial analyses.

Comparative analysis between diagnostic groups

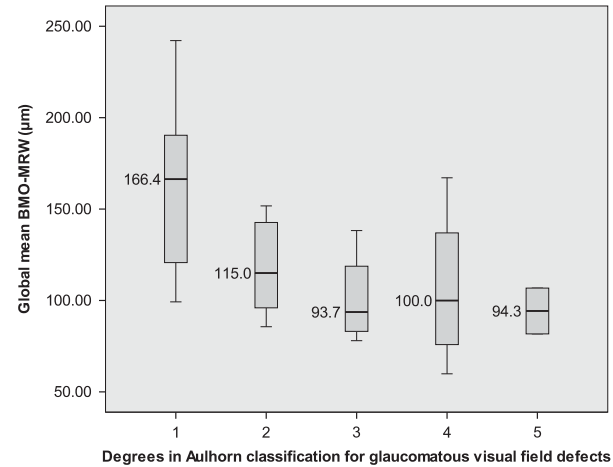In ROC analysis for diagnostic power to discriminate glaucoma patients and non-glaucomatous controls,

BMO-MRW demonstrated the highest area under curve (AUC) at 0.96, while sensitivity at 95% specificity was 84%. Diagnostic power of rim area in CSLT (AUC = 0.91; sensitivity = 60%; $P = 0.01$) and peripapillary RNFLT (AUC = 0.89; sensitivity = 63%; $P = 0.04$) were significantly less powerful to detect glaucoma. There was no statistical significant difference between AUCs of rim area in CSLT and peripapillary RNFLT ($P = 0.6$).

Mean age of glaucoma patients (68.4 years) and non-glaucomatous controls (38.8 years) differed significantly ($P < 0.001$). A subsequent analysis was performed including only patients 45 years of age and older in both groups. In 44 glaucoma patients with macrodiscs and 29 controls, mean age was comparable ($P = 0.06$). In ROC analysis, AUC of BMO-MRW was 0.93, AUC of rim area in CSLT was 0.89 and AUC of RNFLT was 0.83, respectively. While the difference between BMO-MRW and RNLFT remains statistically significant with $P = 0.03$, level of significance was not reached for the difference of BMO-MRW and rim area in CSLT.

Figure 3 displays ROC-analysis for BMO-MRW, RNFL and rim area in CSLT for all glaucoma patients and non-glaucomatous controls. Cutoff points at 95% specificity were 211.8 μm for BMO-MRW, 76.5 μm for RNFL and 1.48 mm^2 for rim area in CSLT.

Discussion

BMO-based SD-OCT of the optic nerve head plays an increasingly important role as diagnostic tool, bearing major advantages compared to previous techniques.[11–13] BMO-MRW showed highest sensitivity in discrimination of glaucoma patients from normal controls out of all
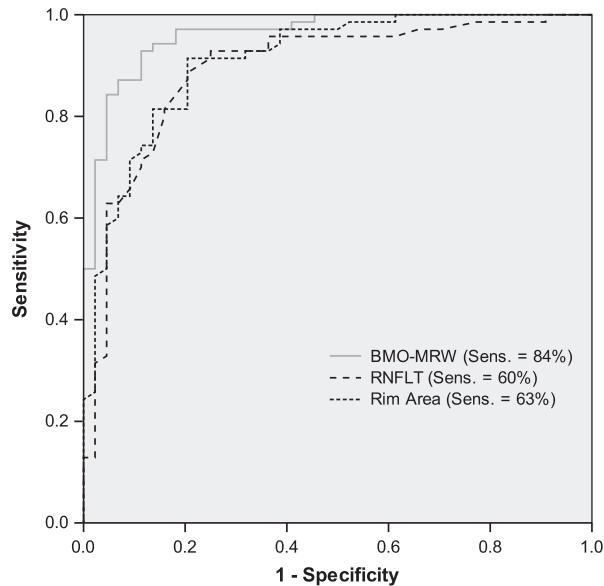
Figure 3 ROC analysis: discrimination of glaucoma patients from normal controls by BMO-MRW, RNFL (OCT) and CSLT rim area with sensitivities at 95%-specificity. Legend: ROC, Receiver Operator Characteristic; BMO-MRW, Bruch's membrane opening-based minimum rim width; RNFLT, Retinal nerve fiber layer thickness; CSLT, confocal scanning laser tomography.

currently clinically available parameters.[13] New morphometric parameters such as BMO-based minimum rim area (BMO-MRA) are currently in evaluation.[4,22] Structure function relationship was analyzed in multiple studies.[14,32–34]

In SD-OCT morphometry, data on special configurations of the optic disc is currently in scope of different research groups, especially for very small or very large discs, myopic discs, tilting of the disc as well as other papillary anomalies. Recently, we have published data on 102 controls in SD-OCT analysis of the optic nerve head in non-glaucomatous large optic discs.[23] For small optic disc as well as for myopic discs, diagnostic power of BMO-based parameters has been analyzed as well.[24,25]

For glaucomatous macrodiscs data was still missing. Our aim was to add OHT and glaucoma patients to the existing database. For non-glaucomatous individuals with macrodiscs BMO-based minimum rim width and RNFLT are thinner.[22] Patients with regular visual field function and ocular hypertension did not show a significant decrease of BMO-MRW or RNFL compared to normal controls.

In the present study, BMO-MRW showed highest sensitivity to discriminate glaucoma patients from normal controls. Unlike in other special disc situations (ie,, myopic discs or microdiscs), peripapillary RNFLT measurement did not seem to represent an additional diagnostic aid as comprising the significantly lowest

AUC. Within the aged-match control group, overall AUCs were higher than in microdiscs.[25] Furthermore, BMO-MRW is more powerful to assess the functional defects in visual field testing compared to the other morphometric parameters RNFLT and rim area in CSLT.[22] Along visual stages in visual field classifications Hodapp-Anderson-Parris and Aulhorn, BMO-MRW decreases significantly with loss of function. An individual, patient-specific predictability of the structure-function relationship is limited due to the large variation within those parameters as well as learning effects in visual field testing.[35]

Limitations of our study include the retrospective study set-up, only one available visual field test result as well as a potential selection bias due to patient exclusion due to data inconsistencies. Epidemiologic and baseline data of the study group reflected a characteristic pattern of glaucoma patients.

In summary, for large optic discs, so called macrodiscs, the BMO-based parameter minimum rim width assessed by SD-OCT has the best diagnostic power to detect glaucoma compared to other clinically available morphometric parameters and reflects best structure-function relationship.

Summary

What was known before
- In very large optic nerve heads diagnosis of glaucoma presents a major challenge for clinicians, as the neuroretinal rim in funduscopy seems thinned. Bruch's membrane opening minimum rim width (BMO-MRW) as well as retinal nerve fiber layer thickness (RNFLT) analysis of the optic nerve head by Bruch's membrane opening (BMO) based spectral domain optical coherence tomography (SD-OCT) increasingly become available for glaucoma detection in clinical practice. Performance of this diagnostic tool in large optic nerve heads has not yet been assessed.

What this study adds
- In macrodiscs, BMO-MRW has the best diagnostic power to discriminate glaucoma patients from normal controls compared to RNFLT and rim area in CSLT. Additionally, BMO-MRW seems to reflect the structure-function relationship better than the other two parameters.

Conflict of interest

The authors declare no conflict of interest.

References

1 Hoffmann EM, Zangwill LM, Crowston JG, Weinreb RN. Optic disk size and glaucoma. *Surv Ophthalmol* 2007; **52**(1): 32–49.

2 Okimoto S, Yamashita K, Shibata T, Kiuchi Y. Morphological features and important parameters of large optic discs for diagnosing glaucoma. *PLoS ONE* 2015; **10**(3): e0118920.

3 Jonas JB, Budde WM. Optic nerve head appearance in juvenile-onset chronic high-pressure glaucoma and normal-pressure glaucoma. *Ophthalmology* 2000; **107**(4): 704–711.

4 Gardiner SK, Ren R, Yang H, Fortune B, Burgoyne CF, Demirel S. A method to estimate the amount of neuroretinal rim tissue in glaucoma: comparison with current methods for measuring rim area. *Am J Ophthalmol* 2014; **157**(3): 540–549 e541-542.

5 Reis AS, O'Leary N, Yang H, Sharpe GP, Nicolela MT, Burgoyne CF et al. Influence of clinically invisible, but optical coherence tomography detected, optic disc margin anatomy on neuroretinal rim evaluation. *Invest Ophthalmol Vis Sci* 2012; **53**(4): 1852–1860.

6 Reis AS, Sharpe GP, Yang H, Nicolela MT, Burgoyne CF, Chauhan BC. Optic disc margin anatomy in patients with glaucoma and normal controls with spectral domain optical coherence tomography. *Ophthalmology* 2012; **119**(4): 738–747.

7 Chen TC. Spectral domain optical coherence tomography in glaucoma: qualitative and quantitative analysis of the optic nerve head and retinal nerve fiber layer (an AOS thesis). *Trans Am Ophthalmol Soc* 2009; **107**: 254–281.

8 Povazay B, Hofer B, Hermann B, Unterhuber A, Morgan JE, Glittenberg C et al. Minimum distance mapping using three-dimensional optical coherence tomography for glaucoma diagnosis. *J Biomed Opt* 2007; **12**(4): 041204.

9 Abramoff MD, Lee K, Niemeijer M, Alward WL, Greenlee EC, Garvin MK et al. Automated segmentation of the cup and rim from spectral domain OCT of the optic nerve head. *Invest Ophthalmol Vis Sci* 2009; **50**(12): 5778–5784.

10 Mwanza JC, Oakley JD, Budenz DL, Anderson DR. Cirrus Optical Coherence Tomography Normative Database Study G. Ability of cirrus HD-OCT optic nerve head parameters to discriminate normal from glaucomatous eyes. *Ophthalmology* 2011; **118**(2): 241–248 e241.

11 Chauhan BC, Burgoyne CF. From clinical examination of the optic disc to clinical assessment of the optic nerve head: a paradigm change. *Am J Ophthalmol* 2013; **156**(2): 218–227 e212.

12 Chauhan BC, Danthurebandara VM, Sharpe GP, Demirel S, Girkin CA, Mardin CY et al. Bruch's membrane opening minimum rim width and retinal nerve fiber layer thickness in a normal white population: a multicenter study. *Ophthalmology* 2015; **122**(9): 1786–1794.

13 Chauhan BC, O'Leary N, Almobarak FA, Reis AS, Yang H, Sharpe GP et al. Enhanced detection of open-angle glaucoma with an anatomically accurate optical coherence tomography-derived neuroretinal rim parameter. *Ophthalmology* 2013; **120**(3): 535–543.

14 Bowd C, Zangwill LM, Medeiros FA, Tavares IM, Hoffmann EM, Bourne RR et al. Structure-function relationships using confocal scanning laser ophthalmoscopy, optical coherence tomography, and scanning laser polarimetry. *Invest Ophthalmol Vis Sci* 2006; **47**(7): 2889–2895.

15 Anderson RS. The psychophysics of glaucoma: improving the structure/function relationship. *Prog Retin Eye Res* 2006; **25**(1): 79–97.

16 Anton A, Yamagishi N, Zangwill L, Sample PA, Weinreb RN. Mapping structural to functional damage in glaucoma with standard automated perimetry and confocal scanning laser ophthalmoscopy. *Am J Ophthalmol* 1998; **125**(4): 436–446.

17 Caprioli J. Correlation of visual function with optic nerve and nerve fiber layer structure in glaucoma. *Surv Ophthalmol* 1989; **33**(Suppl): 319–330.

18 Gardiner SK, Johnson CA, Cioffi GA. Evaluation of the structure-function relationship in glaucoma. *Invest Ophthalmol Vis Sci* 2005; **46**(10): 3712–3717.

19 Garway-Heath DF, Holder GE, Fitzke FW, Hitchings RA. Relationship between electrophysiological, psychophysical, and anatomical measurements in glaucoma. *Invest Ophthalmol Vis Sci* 2002; **43**(7): 2213–2220.

20 Harwerth RS, Carter-Dawson L, Smith EL 3rd, Crawford ML. Scaling the structure–function relationship for clinical perimetry. *Acta Ophthalmol Scand* 2005; **83**(4): 448–455.

21 Schlottmann PG, De Cilla S, Greenfield DS, Caprioli J, Garway-Heath DF. Relationship between visual field sensitivity and retinal nerve fiber layer thickness as measured by scanning laser polarimetry. *Invest Ophthalmol Vis Sci* 2004; **45**(6): 1823–1829.

22 Muth DR, Hirneiss CW. Structure-function relationship between Bruch's membrane opening-based optic nerve head parameters and visual field defects in glaucoma. *Invest Ophthalmol Vis Sci* 2015; **56**(5): 3320–3328.

23 Enders P, Schaub F, Hermann MM, Cursiefen C, Heindl LM. Neuroretinal rim in non-glaucomatous large optic nerve heads: a comparison of confocal scanning laser tomography and spectral domain optical coherence tomography. *Br J Ophthalmol* 2016; **101**(2): 138–142.

24 Malik R, Belliveau AC, Sharpe GP, Shuba LM, Chauhan BC, Nicolela MT. Diagnostic accuracy of optical coherence tomography and scanning laser tomography for identifying glaucoma in myopic eyes. *Ophthalmology* 2016; **123**(6): 1181–1189.

25 Enders P, Schaub F, Nikoluk R, Hermann MM, Heindl LM. The use of Bruch's membrane opening-based optical coherence tomography of the optic nerve head for glaucoma detection in micro-discs. *Br J Ophthalmol* 2017; **101**(4): 530–535.

26 Society EG. *Terminology and Guidelines for Glaucoma*4th ednPubliComm: Savona, Italy, 2014.

27 Aulhorn E. [Subjective examination methods in glaucoma diagnosis]. *Buch Augenarzt* 1976; (69): 128–139.

28 Aulhorn E. [Clinical function test in glaucoma]. *Buch Augenarzt* 1971; **56**: 15–27.

29 Aulhorn E. [Visual field in glaucoma]. *Ophthalmologica* 1969; **158**(5): 469–487.

30 Kymes S. Cost-effectiveness of monotherapy treatment of glaucoma and ocular hypertension with the lipid class of medications. *Am J Ophthalmol* 2006; **142**(2): 354 author reply 354–355.

31 Eichstaedt KE, Kovatch K, Maroof DA. A less conservative method to adjust for familywise error rate in neuropsychological research: the Holm's sequential Bonferroni procedure. *Neurorehabilitation* 2013; **32**(3): 693–696.

32 Pollet-Villard F, Chiquet C, Romanet JP, Noel C, Aptel F. Structure-function relationships with spectral-domain optical coherence tomography retinal nerve fiber layer and optic nerve head measurements. *Invest Ophthalmol Vis Sci* 2014; **55**(5): 2953–2962.

33 Nilforushan N, Nassiri N, Moghimi S, Law SK, Giaconi J, Coleman AL *et al.* Structure-function relationships between spectral-domain OCT and standard achromatic perimetry. *Invest Ophthalmol Vis Sci* 2012; **53**(6): 2740–2748.

34 Lee JR, Jeoung JW, Choi J, Choi JY, Park KH, Kim YD. Structure-function relationships in normal and glaucomatous eyes determined by time- and spectral-domain optical coherence tomography. *Invest Ophthalmol Vis Sci* 2010; **51**(12): 6424–6430.

35 Pierre-Filho Pde T, Gomes PR, Pierre ET, Pierre LM. Learning effect in visual field testing of healthy subjects using Humphrey Matrix frequency doubling technology perimetry. *Eye (Lond)* 2010; **24**(5): 851–856.

Medscape
EDUCATION

Bruch's membrane opening-based optical coherence tomography of the optic nerve head: a useful diagnostic tool to detect glaucoma in macrodiscs

To obtain credit, you should first read the journal article. After reading the article, you should be able to answer the following, related, multiple-choice questions. To complete the questions (with a minimum 75% passing score) and earn continuing medical education (CME) credit, please go to **http://www.medscape.org/journal/eye**. Credit cannot be obtained for tests completed on paper, although you may use the worksheet below to keep a record of your answers.

You must be a registered user on http://www.medscape.org. If you are not registered on http://www.medscape.org, please click on the ``Register'' link on the right hand side of the website.

Only one answer is correct for each question. Once you successfully answer all post-test questions you will be able to view and/or print your certificate. For questions regarding this

activity, contact the accredited provider, CME@medscape.net. For technical assistance, contact CME@medscape.net. American Medical Association's Physician's Recognition Award (AMA PRA) credits are accepted in the US as evidence of participation in CME activities. For further information on this award, please go to https://www.ama-assn.org. The AMA has determined that physicians not licensed in the US who participate in this CME activity are eligible for *AMA PRA Category 1 Credits™*. Through agreements that the AMA has made with agencies in some countries, AMA PRA credit may be acceptable as evidence of participation in CME activities. If you are not licensed in the US, please complete the questions online, print the AMA PRA CME credit certificate, and present it to your national medical association for review.

1. Your patient is a 67-year-old man with a large optic disc and suspected glaucoma. According to the case-control, cross-sectional study by Enders and colleagues, which of the following statements about morphometric measurements and diagnostic performance for glaucoma detection in macrodiscs by Bruch's membrane opening (BMO)-based spectral domain-optical coherence tomography (SD-OCT) compared with margin-based confocal scanning laser tomography (CSLT) of the optic nerve head (ONH) is *correct*?

   A   Receiver operating characteristic (ROC) analysis showed that diagnostic power to differentiate patients with glaucoma from healthy control participants was highest for rim area on CSLT
   B   For BMO-minimum rim width (MRW), ROC area under curve (AUC) was 0.96; sensitivity was 95%; and specificity was 82%
   C   Compared with healthy control participants, patients with normal visual field function and ocular hypertension had significant decreases in BMO-MRW and retinal nerve fiber layer thickness (RNFLT)
   D   In an age-matched control group, diagnostic performance of these tests was better in patients with microdiscs than in those with macrodiscs

2. According to the case-control, cross-sectional study by Enders and colleagues, which of the following statements about correlation of these morphometric measures (SD-OCT and CSLT) with visual field function is *correct*?

   A   BMO-MRW did not decrease significantly as a function of increasing visual field loss
   B   RNFLT was more highly correlated with visual field function than was global BMO-MRW or rim area in CSLT
   C   BMO-MRW accurately predicted visual field loss for individual patients with glaucoma
   D   BMO-MRW seems to reflect the structure-function relationship better than RNFLT and rim area in CSLT

3. According to the case-control, cross-sectional study by Enders and colleagues, which of the following statements about the clinical implications of these findings regarding morphometric measures in macrodiscs of glaucomatous and non-glaucomatous eyes is *correct*?

   A   For macrodiscs, the BMO-based parameter MRW on SD-OCT has the best diagnostic power to detect glaucoma vs other clinically available morphometric parameters
   B   Peripapillary RNFLT measurement adds significantly to diagnostic power for glaucoma in patients with macrodiscs
   C   Peripapillary RNFLT measurement is not helpful to diagnose glaucoma in patients with myopic discs
   D   No other BMO-based morphometric parameters are currently being tested